J|A|C|S ARTICLES

Published on Web 09/28/2009

Human Insulin-Degrading Enzyme Working Mechanism

Orazio Amata, Tiziana Marino, Nino Russo,* and Marirosa Toscano

Dipartimento di Chimica and Centro di Calcolo ad Alte Prestazioni per Elaborazioni Parallele e Distribuite-Centro d'Eccellenza MURST, Universita' della Calabria, I-87030 Arcavacata di Rende (CS), Italy

Received May 7, 2009; E-mail: nrusso@unical.it

Abstract: The possible mechanism by which the insulin-degrading enzyme (IDE) zinc-binding protease carries out its catalytic function toward two peptides of different length, simulating a portion of B chain of insulin, was investigated on an enzymatic model consisting of 130 /159 atoms, using the density functional theory method and the hybrid exchange−correlation functional B3LYP in gas phase and in the protein environment. Based on the geometry and relative stabilities of minima and transition states on the potential energy profiles, we determined that proteolysis reaction is exothermic and proceeds quickly as the barrier in the rate-limiting step falls widely within the range of values expected for an enzymatic catalysis, both in vacuum and in protein medium.

Introduction

Insulin-degrading enzyme (IDE), also known as insulysin, is a highly conserved M16A Zn^{2+}-metalloprotease found in bacteria, fungi, plants, and animals.[1] IDE is unusual in its high affinity for substrates that can be highly diverse in sequence and structure. It also contains an inverted zinc−metalloprotease core motif (HXXEH) located within 200 residues of the N-terminal. This is the reason IDE can be numbered among the "inverzincins" family.

IDE was first identified by its ability to degrade the A and B chains of the hormone insulin, mainly at the sites Leu13-Tyr14 and Tyr14-Gln15 (A chain) and Ser9-His10, His10-Leu11, Glu13-Ala14, Tyr15-Leu16, and Phe25-Tyr26 (B chain).[2] This discovery suggested IDE shares a high degree of homology to pitrilysin, a bacterial protease, and a probable similar proteolytic mechanism.[3] In fact, the enzymes of the M16A subfamily are highly related in primary sequence. Human IDE and pitrilysin have, for example, about 30% identity.[3] This similarity generally extends throughout the entire length of these proteins but is often higher in the N-terminal half.

Interest in IDE was stimulated by the discovery that it can degrade amyloid β (Aβ), a peptide involved in the pathogenesis of Alzheimer's disease, which is the leading cause of dementia affecting a large proportion of the elderly population worldwide.[4−9] In fact, a hypothesized mechanism of this disease assigns a prominent role as causative agent to the hydrophobic peptide Aβ, which forms quaternary structures that in turn, by an unknown mechanism, cause neuronal death. Numerous in vitro and in vivo studies showed correlations between IDE, Aβ degradation, and Alzheimer's disease.[4−9]

Some researchers studied mice that were missing insulysin gene activity.[10,11] They found that the insulysin enzyme degrades not only insulin but also amyloid β peptides. In addition, even a partial decrease in insulysin activity was found to increase amyloid β peptide levels in the brain.[10]

By examining individuals affected by inherited forms of Alzheimer's, a reduction in both IDE expression and catalytic activity was discovered.[12,13] Today the role of IDE in this disease is quite clear; however, the biological functions of IDE as well as many M16A enzymes remain largely uncharacterized. The fact that IDE is localized in the cytosol, peroxisomes, endosomes, proteasome complexes, and in the surface of cerebrovascular endothelial cells suggests these functions may be varied.[14,15]

(1) Mirsky, L. A.; Broth-Kahn, R. H. *Arch. Biochem.* **1949**, *20*, 1.
(2) Duckworth, W. C. *Endocrinol. Rev.* **1988**, *9*, 319.
(3) Alper, B. J.; Nienow, T. E.; Schmidt, W. K. *Biochem. J.* **2006**, *398*, 145.
(4) Morelli, L.; Llovera, R. E.; Alonso, L. G.; Frangione, B.; de Prat-Gay, G.; Ghiso, J.; Castaño, E. M. *Biochem. Biophys. Res. Commun.* **2005**, *332*, 808.
(5) Farris, W.; Leissring, M. A.; Hemming, M. L.; Chang, A. Y.; Selkoe, D. J. *Biochemistry* **2005**, *44*, 6513.
(6) Llovera, R. E.; de Tullio, M.; Alonso, L. G.; Leissring, M. A.; Kaufman, S. B.; Roher, A. E.; de Prat-Gay, G.; Morelli, L.; Castaño, E. M. *J. Biol. Chem.* **2008**, *283*, 17039.
(7) Zhao, L.; Teter, B.; Morihara, T.; Lim, G. P.; Ambegaokar, S. S.; Ubeda, O. J.; Frautschy, S. A.; Cole, G. M. *J. Neurosci.* **2004**, *24*, 11120.
(8) Qiu, W. Q.; Folstein, M. F. *Neurobiol. Aging* **2007**, *27*, 190.
(9) Hersh, L. B. *Cell. Mol. Life Sci.* **2006**, *63*, 2432.
(10) Farris, W.; Mansourian, S.; Chang, Y.; Lindsley, L.; Eckman, E. A.; Frosch, M. P.; Eckman, C. B.; Tanzi, R. E.; Selkoe, D. J.; Guenette, S. *Proc. Natl. Acad. Sci. U.S.A.* **2003**, *100*, 4162.
(11) Miller, B. C.; Eckman, E. A.; Sambamurti, K.; Dobbs, N.; Chow, K. M.; Eckman, C. B.; Hersh, L. B.; Thiele, D. L. *Proc. Natl. Acad. Sci. U.S.A.* **2003**, *100*, 6221.
(12) Cook, D. G.; Leverenz, J. B.; McMillan, P. J.; Kulstad, J. J.; Ericksen, S.; Roth, R. A.; Schellenberg, G. D.; Jin, L. W.; Kovacina, K. S.; Craft, S. *Am. J. Pathol.* **2003**, *162*, 313.
(13) Kim, M.; Hersh, L. B.; Leissring, M. A.; Ingelsson, M.; Matsui, T.; Farris, W.; Lu, A.; Hyman, B. T.; Selkoe, D. J.; Bertram, L.; Tanzi, R. E. *J. Biol. Chem.* **2007**, *282*, 7825.
(14) Duckworth, W. C.; Bennett, R. G.; Hamel, F. G. *Endocr. Rev.* **1988**, *19*, 608.
(15) Lynch, J. A.; George, A. M.; Eisenhauer, P. B.; Conn, K.; Gao, W.; Carreras, I.; Wells, J. M.; McKee, A.; Ullman, M. D.; Fine, R. E. *J. Neurosci. Res.* **2006**, *83*, 1262.

10.1021/ja9037142 CCC: $40.75

From studies addressed to the determination of IDE crystal structure,[16] it was ascertained that the zinc-binding active site stays within a proteolytic cavity formed by defined N- and C-terminal units joined by a loop involving 28 amino acid residues.

The catalytic chamber is large enough to selectively bind and degrade substrates such as insulin and amyloid β (Aβ), composed of 51 and 39−43 amino acid residues, respectively. In these cases the enzyme uses an exosite that lies about 30 Å away from the catalytic center to anchor the N-terminus of peptides. This serves to locate suitably the substrate facilitating the cleavage at the catalytic site. However, for substrates less than 12 amino acids long, the anchoring and degrading mechanism is not known since it is impossible for shorter peptides to bind the exosite and the catalytic center at the same time. In any case, recent studies,[17,18] showed that the rate of catalysis of IDE is higher toward short substrates (>2000 s^{-1}) than toward long substrates such as insulin (about 0.56 min^{-1}).

IDE can exist in two conformations. The first one is an open conformation that allows entry of substrates and exit of products. The other one is a closed conformation, in which the active site, contained within the chamber formed by the two concave domains, is harder to access. The switch from the closed to the open conformation favors the entry of the substrates into the catalytic cavity. In fact, if mutations prevent the closed conformation, a significant increase (about 40-fold) in catalytic efficiency of the enzyme is revealed.[16] This observation suggested a possible therapy for Alzheimer's consisting of changing the conformational preference of IDE to the open state. This should increase Aβ degradation, preventing aggregation and neuronal death.

However, this problem should be addressed carefully since mutation of the active-site residues of IDE can not only reduce catalytic activity but also cause local conformation changes that alter the allosteric properties of the enzyme.[19]

Studies present in literature explored many aspects concerning IDE,[1−24] but none of them deals with the mechanistic details of the proteolysis performed by this enzyme.

In this work, we used density functional theory to explore the catalytic mechanism of IDE in the breaking of two peptides of different lengths, representing a portion of the B chain of insulin hormone. We hoped our work would provide some valuable fundamental insights into the behavior of this enzyme.

Computational Details

Density functional theory (DFT) calculations were carried out with the Gaussian03 program.[25] The geometries of reactants, intermediates, transition states, and products were fully optimized via diverse treatment for atoms belonging to the first and second coordination shells of catalytic zinc ion. The B3LYP/6-31+G(d,p) and B3LYP/6-31G(d,p) levels were used, respectively.[26−29] The Stuttgart/Dresden (SDD) pseudopotential was applied to describe the metal center.[30,31] During geometry optimization, some degrees of freedom of the molecular system were constrained to maintain a reasonable approximation to the active-site crystal geometry. This is realized by fixing the atoms to their crystallographic positions where truncation is done. With this procedure the risk exists that the model can become too rigid with significant effects on the energetics. However, it was demonstrated[32] that these effects usually do not alter any conclusion concerning the working mechanism of the enzyme.

For each species, vibration analyses were performed to obtain the zero-point energies (ZPE) and verify whether each is a minimum or a transition state on the potential energy surfaces (PES). Intrinsic reaction coordinate (IRC) calculations were performed to confirm that a given transition state connects a particular couple of consecutive minima.[33,34]

To consider solvent effects, the single-point energies of all structures were calculated with the self-consistent reaction field (SCRF) conductorlike polarizable continuum model (CPCM) method[35,36] using a dielectric constant value $\varepsilon = 4$ that takes into account the coupled effect of the protein itself and the water medium surrounding the protein, according to our previous experience and literature suggestions.[37−47] United atom topological model (UA0) applied on atomic radii of the UFF force field was used to build the cavity, in the gas-phase equilibrium geometry.[48]

By manual cutting of the crystal structure [PDB code 2G54] of IDE[16] in complex with a portion of insulin B chain, two models for the active site were built up, which consist of 130 and 159 atoms; both models have a total charge equal to zero.

A quite complete identification of zinc ion ligands was done by Perlman and Rosner[49] in 1994. In this work, on the basis of

(16) Shen, Y.; Joachimiak, A.; Rosner, M. R.; Tang, W. J. *Nature* **2006**, *443*, 870.
(17) Malito, E.; Ralat, L. A.; Manolopoulou, M.; Tsay, J. L.; Wadlingthon, N. L.; Tang, W.-J. *Biochemistry* **2008**, *47*, 12822.
(18) Song, E.-S.; Juliano, A. M.; Juliano, L.; Hersh, L. B. *J. Biol. Chem.* **2003**, *278*, 49789.
(19) Song, E.-S.; Daily, A.; Fried, M. G.; Juliano, A. M.; Juliano, L.; Hersh, L. B. *J. Biol. Chem.* **2005**, *280*, 17701.
(20) Ciaccio, C.; Tundo, G. R.; Grasso, G.; Spoto, G.; Marasco, D.; Ruvo, M.; Gioia, M.; Rizzarelli, E.; Coletta, M. *J. Mol. Biol.* **2009**, *385*, 1556.
(21) Grasso, G.; Rizzarelli, E.; Spoto, G. *J. Mass Spectrom.* **2009**, *44*, 735−741 (DOI 10.1002/jms.1550).
(22) Alper, B. J.; Schmidt, W. K. *J. Neurosci. Methods* **2009**, *178*, 40.
(23) Evin, G.; Weidemann, A. *Peptides* **2002**, *23*, 1285.
(24) Neant-Fery, M.; Garcia-Ordoñez, R. D.; Logan, T. P.; Selkoe, D. J.; Li, L.; Reinstatler, L.; Leissring, M. A. *Proc. Natl. Acad. Sci. U.S.A.* **2008**, *105*, 9582.
(25) Frisch, M. J., *Gaussian 03*; Gaussian, Inc.: Pittsburgh, PA, 2003.
(26) Becke, A. D. *J. Chem. Phys.* **1993**, *98*, 5648.
(27) Lee, C.; Yang, W.; Parr, R. G. *Phys. Rev. B* **1988**, *37*, 785.
(28) Becke, A. D. *J. Chem. Phys.* **1993**, *98*, 1372.
(29) Becke, A. D. *Phys. Rev. B* **1988**, *38*, 3098.
(30) Dolg, M.; Wedig, U.; Stoll, H.; Preuss, H. *J. Chem. Phys.* **1987**, *86*, 866.
(31) Andrae, D.; Haussermann, U.; Dolg, M.; Stoll, H.; Preuss, H. *Theor. Chim. Acta* **1990**, *77*, 123.
(32) Chen, S.-L.; Fang, W.-H.; Himo, F. *Theor. Chem. Acc.* **2008**, *120*, 515.
(33) Gonzalez, C.; Schlegel, H. B. *J. Chem. Phys.* **1989**, *90*, 2154.
(34) Gonzalez, C.; Schlegel, H. B. *J. Phys. Chem.* **1990**, *94*, 5523.
(35) Barone, V.; Cossi, M. *J. Phys. Chem. A* **1998**, *102*, 1995.
(36) Cossi, M.; Rega, N.; Scalmani, G.; Barone, V. *J. Comput. Chem.* **2003**, *24*, 669.
(37) Leopoldini, M.; Russo, N.; Toscano, M. *J. Phys. Chem. B* **2006**, *110*, 1063.
(38) Marino, T.; Russo, N.; Toscano, M. *J. Am. Chem. Soc.* **2005**, *127*, 4242.
(39) Siegbahn, P. E. M.; Blomberg, M. R. A. *Chem. Rev.* **2000**, *100*, 421.
(40) Noodleman, L.; Lovell, T.; Han, W. G.; Li, J.; Himo, F. *Chem. Rev.* **2004**, *104*, 459.
(41) Leopoldini, M.; Russo, N.; Toscano, M. *J. Am. Chem. Soc.* **2007**, *129*, 7776.
(42) Leopoldini, M.; Russo, N.; Toscano, M.; Dulak, M.; Wesoloski, A. T. *Chem.—Eur. J.* **2006**, *12*, 2532.
(43) Leopoldini, M.; Russo, N.; Toscano, M. *Chem.—Eur. J.* **2009**, *15*, 8026−8036.
(44) Leopoldini, T.; Marino, N.; Toscano, M. *Theor. Chem. Acc.* **2008**, *120*, 459.
(45) Chen, S.-L.; Marino, T.; Fang, W.-H.; Russo, N.; Himo, F. *J. Phys.Chem. B* **2008**, *112*, 2494.
(46) Ramos, M. J.; Fernandes, P. A. *Acc. Chem. Res.* **2008**, *41*, 689.
(47) Russo, N.; Leopoldini, M.; Toscano, M. *Chem.—Eur. J.* **2007**, *13*, 2109.
(48) Barone, V.; Cossi, M.; Menucci, B.; Tomasi, J. *J. Chem. Phys.* **1997**, *107*, 3210.
(49) Perlman, R. K.; Rosner, M. R. *J. Biol. Chem.* **1994**, *269*, 33140.

Scheme 1. Active-Site Model of IDE

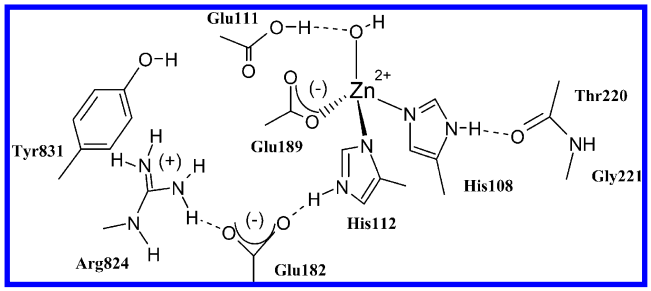

mutagenesis of some potential zinc-binding residues, it was established that metal center in human IDE is chelated by His108, His112, and Glu189. The more external residues Tyr831, Glu111, Thr220, Gly221, Glu182, and Arg824 were also determined. Among these last residues, mainly Glu182, although not directly involved as metal ligand, plays a fundamental role in influencing metal recognition and binding by zinc proteins.[49] Glu111 was recognized as the residue that deprotonates the water molecule that completes the coordination sphere of zinc. In fact, in active sites of enzymes, zinc is typically bound to a water molecule involved in nucleophilic attack on the peptide carbonyl. Zinc ion seems to play a double role. It is not only the catalytic center but also contributes to the stabilization of tertiary structure of the proteins by bridging groups into a correct reciprocal orientation. This is confirmed by the fact that its removal, performed by chelation or mutagenesis, entails conformational changes and catalytic activity loss.[49]

In the active-site model we used, illustrated in Scheme 1, imidazole ring, acetate group, guanidinium moiety, and *p*-methylphenol substitute for histidine, glutamate, arginine, and tyrosine amino acid residues, respectively. A $CH_3CONHCH_3$ peptide bond was used to simulate the linking between threonine and glycine. Substrate CH_3NH-Leu-Tyr-Leu-$CONHCH_3$ present in the PDB was modeled by a CH_3NH-Ala-Ala-Ala-$CONHCH_3$ peptide in the first model (130 atoms), while it was considered as such in the second one (159 atoms).

Results and Discussion

As mentioned before, in spite of the enormous attention that has been dedicated to the study of IDE over the past decade, several crucial aspects in the catalytic mechanism of this enzyme remain unexplained. IDE cleaves insulin B chain as well as amyloid β at several sites;[16] however, our study seeks to determine not the particular cleavage site but rather how this cleavage occurs. The steps involved in the whole process and determined through our calculations are collected in Scheme 2. Structural details of each intermediate and transition state along the reaction path in the presence of CH_3NH-Ala-Ala-Ala-$CONHCH_3$ peptide substrate are given in Figures 1−3. Energetic profiles in gas phase and in protein environment can be found in Figure 4a.

The optimized structure of enzyme−substrate complex (ES) is reported in Figure 1. Comparison of some B3LYP interatomic distances with experimental values (given in parentheses in Figure 1) confirms that the computational approach used is quite reliable. We can note, for example, the similarity between theoretical and experimental values of the coordination distances of His108 (2.060 vs 2.003 Å), His112 (1.974 vs 1.998 Å), Glu189 (2.033 vs 2.047 Å), and deprotonated water (1.963 vs 2.090 Å) to zinc ion.[16,49] Furthermore, as expected, the role of Glu111 as general base is highlighted by the presence of its hydroxyl hydrogen atom placed almost halfway between this residue and the zinc-bound hydroxide ($O_3H-O_1H = 1.483$ Å).

Substrate, in ES, is kept in an orientation suitable so that a carbonyl group of the peptide can undergo nucleophilic attack by the hydroxide linked to the zinc ion. This orientation is allowed by the hydrogen bonds that Arg824, Tyr831, and Glu189 residues establish with two carbonyl oxygens and one amide hydrogen of substrate. This agrees with the role assigned to these amino acids in previous experimental works.[16,50]

The other two hydrogen bonds, formed by Glu182 with His112 and by the pair Thr220-Gly221 with His118, have a stabilizing effect on the whole structure of enzyme−substrate complex. The distance between the nucleophile and the carbonyl attack site, in ES, is still quite long ($C_1-O_1 = 2.894$ Å) but in any case of the same order of those computed for other enzymes[38,41,51] in which the nuclephilic attack is performed by a zinc-bound hydroxide. In fact, zinc(II) is an intermediate acid in Pearson's hard and soft acid and bases (HSAB), which usually imparts to the hydroxyl oxygen a moderate nucleophilicity that prevents the immediate activation of the substrate.

The first step of the mechanism that we propose consists of the mentioned nuclephilic attack that materializes in the intermediate INT1 through the transition state TS1, whose optimized structure is presented in Figure 2. TS1 is characterized by a pentacoordinated zinc ion because of the incipient formation of a bond with the nearest carbonyl oxygen of the substrate ($Zn^{2+}-O_2 = 2.225$ Å). Simultaneously, the pre-existing $Zn^{2+}-O_1H$ bond lengthens by 0.237 Å with respect to its value in ES complex. A lengthening by about 0.08 and 0.07 Å can be observed also for C_1-O_2 carbonyl and the C_1-N_1 distance in the substrate, respectively. TS1 transition state was confirmed to be a first-order saddle point with an imaginary frequency of $107i$ cm^{-1} that is associated with the stretching vibrational mode of the incoming $Zn^{2+}-O_2$ bond. Hydrogen-bond interactions present in the enzyme−substrate complex are all retained, although with values different from those obtained in the previous step (see Figures 1 and 2). TS1 lies at 17.2 kcal/mol above ES, as can be observed from Figure 4a. The barrier for nucleophilic attack in the gas phase is thus quite in line with those encountered in enzymatic catalysis. Upon addition of protein environment effects, the barrier becomes slightly lower (15.9 kcal/mol), suggesting a slight stabilization due to the low polarity of solvent.

In the next step, the intermediate INT1 is formed (see Figure 2). In this species, we can note that the zinc-bound hydroxide is completely transferred on the carbonyl carbon of substrate ($C_1-O_1H = 1.540$ Å) as a consequence of the $Zn^{2+}-O_1H$ (2.405 Å) bond breaking. From the energetic point of view, INT1 is found at about 0.1 and 0.2 kcal/mol below TS1 in gas phase and in solvent, respectively. This light difference in the energy values can be due to the great resemblance of two stationary points. In fact, the change of geometrical parameters in going from TS1 to INT1 is on the whole very small.

Moving along the gas-phase potential energy profile, a new transition state TS2 is encountered that lies at 4.2 kcal/mol above INT1 (see Figure 4a). In TS2, the imaginary frequency of $181.i$ cm^{-1} describes the rotation of Glu111 residue that assumes the right disposition to form two hydrogen bonds with the amide nitrogen ($HN_1-HO_3 = 2.238$ Å) and the −OH group ($C_1O_1-HO_4 = 2.120$ Å) linked to the carbon atom of substrate, thus behaving as hydrogen donor and acceptor, simultaneously. The formation of the second cited bond favors the re-establish-

(50) Maskos, K. In *Handbook of Metalloproteins*; Messerschmidt, A., Dode, W., Cygler, M., Eds.; John Wiley & Sons: New York, 2004; pp 190−198.
(51) Bottoni, A.; Lanza, C. Z.; Miscione, G. P.; Spinelli, D. *J. Am. Chem. Soc.* **2004**, *126*, 1542.

Scheme 2. Chemical Steps in the Proposed Mechanism of Proteolysis by IDE

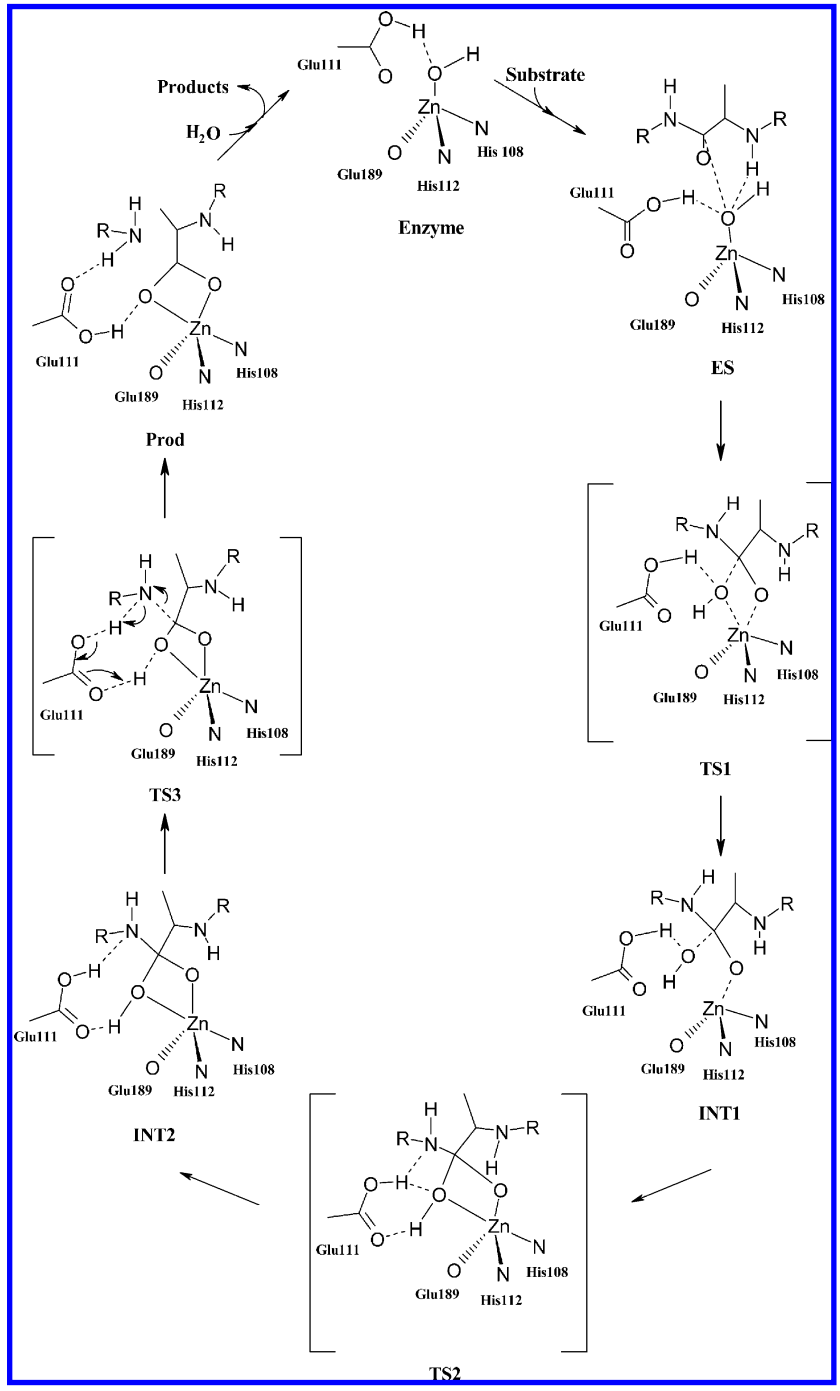

ment of the $Zn^{2+}-O_1H$ bond (2.285 Å) broken previously at the INT1 level. The peptide N_1-C_1 bond of the substrate continues gradually lengthening in all the stationary points along the reaction path. The hydrogen bonds between the Arg824 residue and the terminal CO group of the substrate assume in TS2 values quite different from those observed in the other structures. The same occurs for the hydrogen bond between the hydrogen of His108 and the carbonyl oxygen of the simple moiety used to simulate Thr220 and Gly221 amino acids (see Figure 2).

Solvation effects do not significantly change the energetics of the step that leads from INT1 to TS2. The barrier of 4.2 kcal/mol calculated in gas phase is only 0.7 kcal/mol lower in a protein environment.

The intermediate INT2 (see Figure 3) that originates from TS2 shows the strengthening of the hydrogen bonds between Glu111 and the substrate. HN_1-HO_3 and $C_1O_1-HO_4$ distances are now 1.756 and 1.722 Å long, respectively. The peptide N_1-C_1 bond that must be broken in the substrate further lengthens by 0.05 Å. All other hydrogen bonds are retained with values that in some case are slightly different from those present in TS2 because of the reorganization of amino acid residues.

In gas phase, INT2 is found to be more stable than TS2 by about 2.0 kcal/mol. On the contrary, in a protein medium, it becomes 4.4 kcal/mol more stable than TS2. A look at the previous part of the path, in which the relative differences in energy between the various minima and transition states appear to be quite small, indicates now a moderately larger solvent

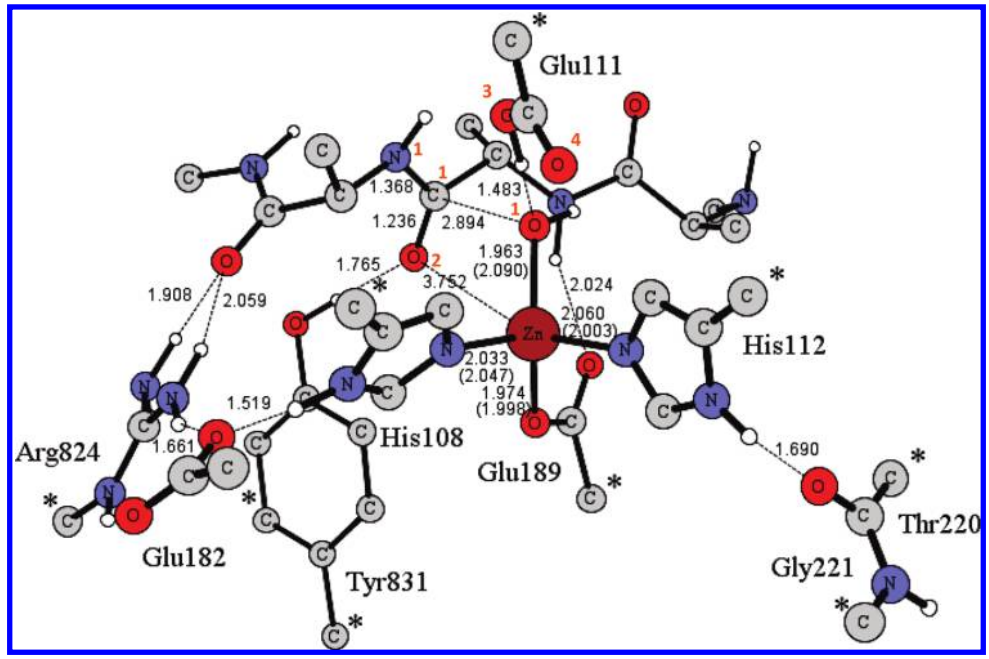

Figure 1. Optimized structure of the enzyme−CH_3NH-Ala-Ala-Ala-$CONHCH_3$ substrate complex. Only the most significant hydrogen atoms are reported. Stars indicate the atoms kept fixed to their crystallographic positions during optimizations. Atoms directly involved in the catalytic reaction are numbered in orange (in the other figures this numeration is not reported but it the same). Distances are in angstroms. Values in parentheses come from refs 16 and 48.

effect. Large solvent effects usually occur when charges are created or quenched in the proximity of the edge of the quantum active-site model. So, in the present case, we could attribute them to the major negative charge distributed on the Glu111 residue oxygens in INT2 rather than in INT1 and due to the incipient hydroxyl proton transfer on N_1 atom of substrate.

The following point on the reaction path is the transition state TS3 (see Figure 3). The most significant peculiarities in this species are the definitive shift of the proton from Glu111 to the amide nitrogen of the substrate and the consistent lengthening (about 0.2 Å) of peptide N_1—C_1 bond. Besides, both these processes are accompanied by the breaking of the Zn^{2+}-O_2C_1 bond that restores the tetrahedral environment around the catalytic ion.

Imaginary frequency visualization program shows that the three chemical events mentioned above occur simultaneously at 158*i* cm^{-1}. All other stabilizing interactions are always present and the values orf distances can be found in Figure 3.

As in other catalytic cycles[43,45] described by flat energetic profiles involving species of comparable energy, we have found that TS3 lies 1.4 kcal/mol below INT2, in gas phase. When the solvent effect is added, the difference in energy becomes 2.2 kcal/mol, with TS3 again more stable than INT2. Usually, on the basis of similar results, conclusions were drawn that hypothesize that nucleophilic addition and the protonation of peptide amide nitrogen may occur as a single step in the catalytic process. In other words, we could say that the protonation of amide nitrogen is a very fast process.

The final species on the path is the product PROD (see Figure 3). As a consequence of transfer of the proton of Glu111 onto the amide nitrogen of substrate that occurred in TS3, the peptide N_1—C_1 bond is broken, as is evident from the distance value of 4.290 Å.

One of the peptide fragments (C-terminus) remains neutral and anchored to the Arg824 residue, while the other one (N-terminus) is still linked to the zinc ion. In PROD, Glu111 is in the protonated state. To restore the active form of the enzyme, some residue present in the protein environment should snatch the proton of Glu111 before the entry of a new water molecule in order to allow this amino acid to carry out its base function. However, this aspect is not thus important in our investigation, since our aim was to describe in detail the peptide hydrolysis phase.

PROD lies 7.0 kcal/mol below the enzyme−substrate complex so that the reaction is exothermic. The exothermicity increases in solvent by 5.8 kcal/mol (see Figure 4a).

A look at the whole reaction path indicates that the rate-determining step in this process is the nucleophilic addition and that after this point the catalytic event should proceed without particular obstacles. Considering the particular location of TS3, that is, the moment in which the protonation of amide nitrogen of peptide substrate occurs, and the small energetic expense to cross TS2, we could hypothesize after TS1 a descendent pathway.

Results just described concern our first model in which the CH_3NH-Leu-Tyr-Leu-$CONHCH_3$ substrate present in the PDB was simulated by a CH_3NH-Ala-Ala-Ala-$CONHCH_3$ peptide, having replaced all side chains by methyl groups. In order to verify that such a simplification does not affect the specificity of the substrate recognized by the enzyme, all calculations were redone removing this simplification and reintroducing all the side chains of substrate amino acids residues.

Results indicate that reaction occurs following the same steps and the same mechanism as in the previous case. All stationary points of the new energetic path (reported in Figure 4b) show geometrical parameters that, although similar to those of the corresponding structures obtained in the case of the smaller peptide substrate, present some slight differences due essentially to the higher steric hindrance. The optimized structure of the enzyme−CH_3NH-Leu-Tyr-Leu-$CONHCH_3$ substrate complex and geometrical features of its stationary points can be found in Figures S1−S3 in Supporting Information.

As can be noted, the energetic paths of Figure 4a,b for the two examined peptides substrates are evidently comparable. TS1, which also in this second case represents the rate-determining step of the reaction, is lower by only 1.5 kcal/mol (in gas phase)

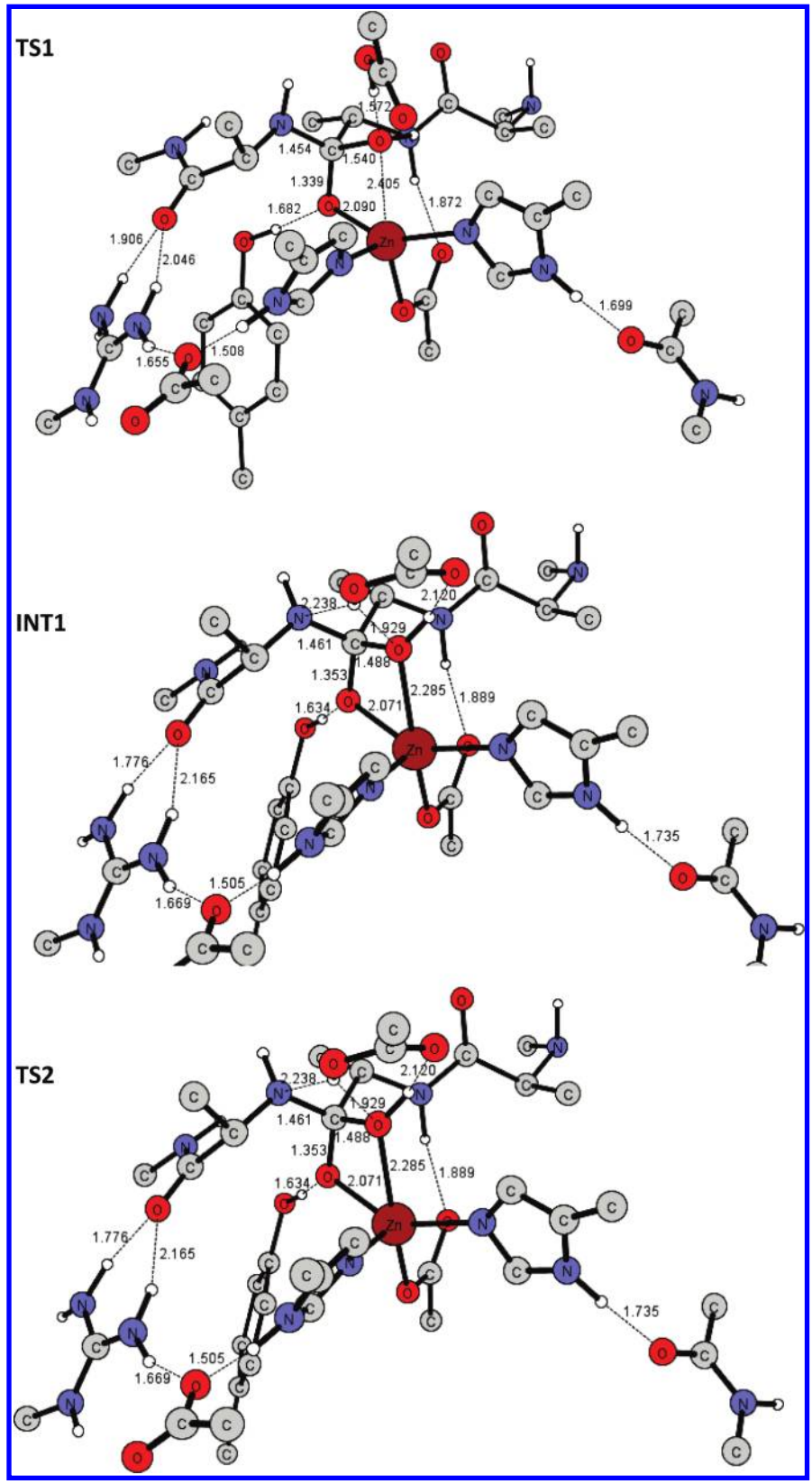

Figure 2. Stationary points (TS1, INT1, and TS2) on the IDE energetic profile for CH_3NH-Ala-Ala-Ala-$CONHCH_3$ substrate.

and 0.3 kcal/mol (in proteinlike medium) with respect to the corresponding TS1 obtained with the substrate model. The vibrational frequency of $120i$ cm^{-1} appears to be associated to the stretching mode of the $Zn^{2+}-O_2$ bond as before.

The similarity between the relative energy values of TS1 and the following INT1 found in the path of Figure 4a is proposed again in the path of Figure 4b and can be explained still by their structural resemblance.

The rotation of Glu111 residue occurs at a frequency value of $153i$ cm^{-1} and requires an expense of 6.3 and 5 kcal/mol in gas and in protein phase, respectively. These values are slightly

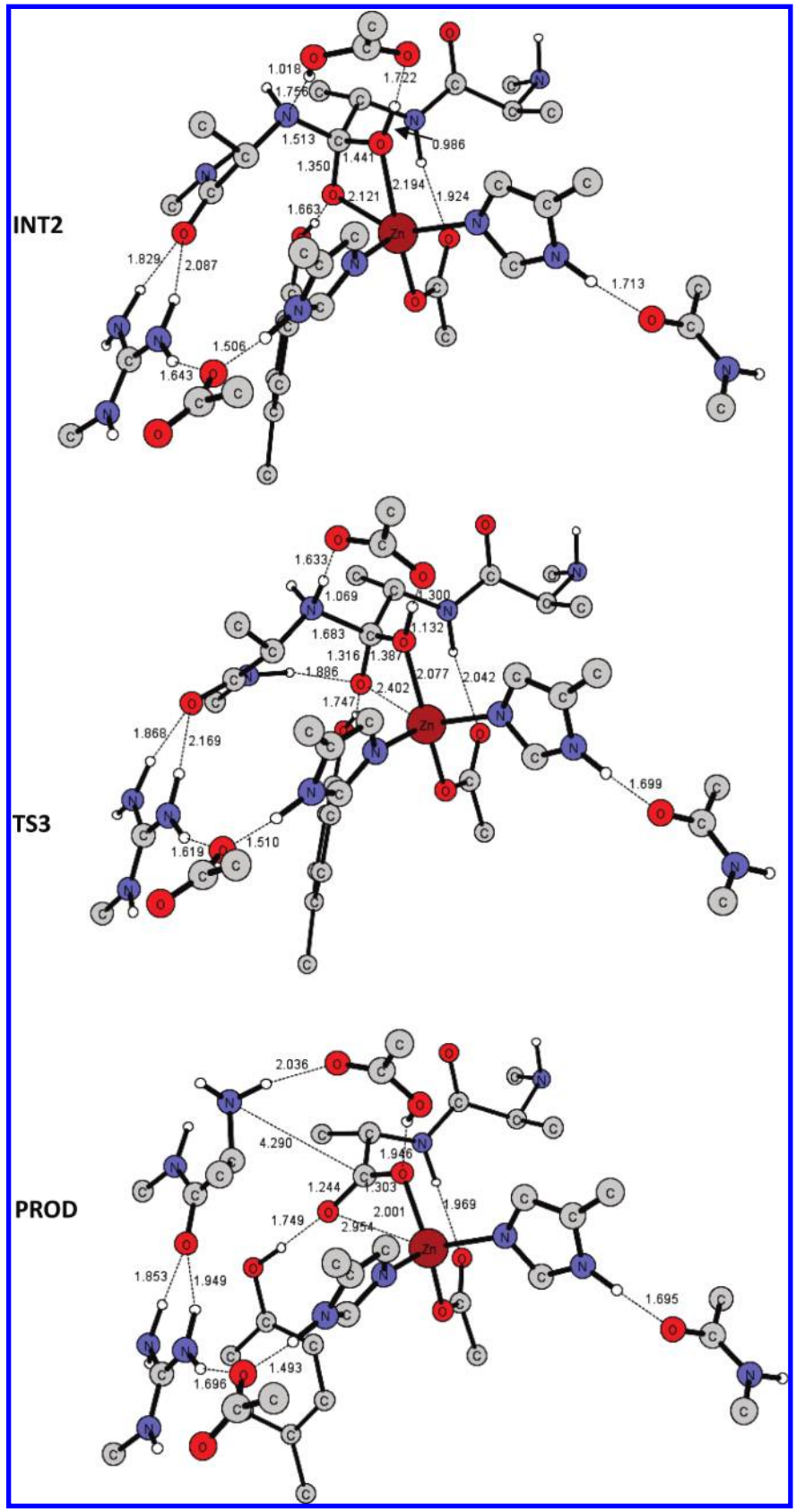

Figure 3. Stationary points (INT2, TS3, and PROD) on the IDE energetic profile for CH_3NH-Ala-Ala-Ala-$CONHCH_3$ substrate.

higher than those obtained with the smaller substrate but it seems quite reasonable that the side chains present in the larger substrate can to some extent block Glu111 to realize the proper orientation to form the two hydrogen bonds with the amide nitrogen and the −OH group linked to the carbon atom of substrate. This in turn, as mentioned before, allows re-formation of the $Zn^{2+}-O_1H$ bond and the lengthening of the peptide N_1-C_1 bond of the substrate.

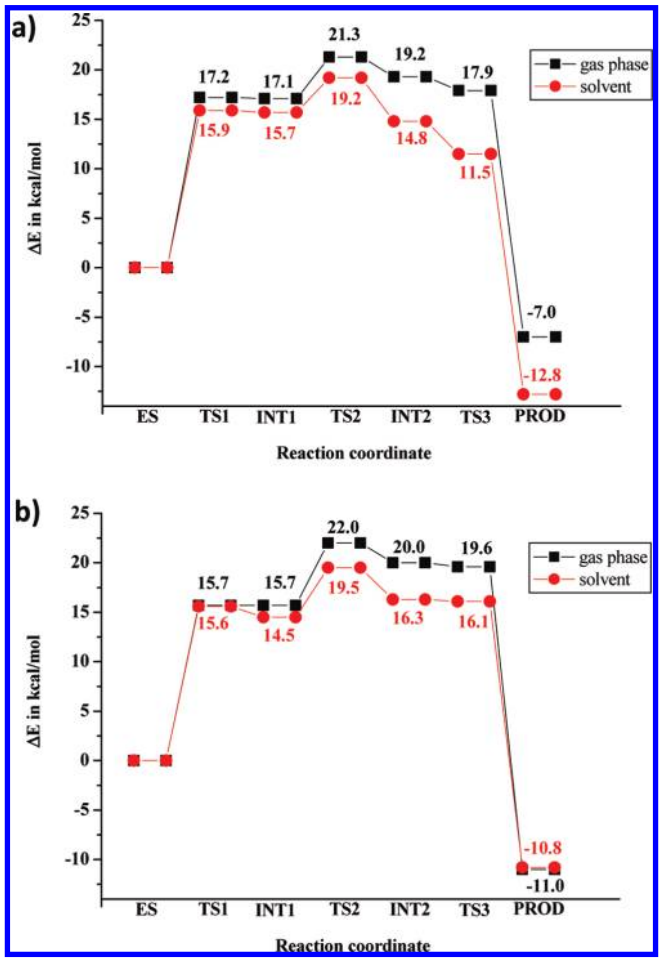

Figure 4. Energetic profile of proteolysis mechanism of IDE toward (a) CH_3NH-Ala-Ala-Ala-$CONHCH_3$ and (b) CH_3NH-Leu-Tyr-Leu-$CONHCH_3$ substrates.

The energy difference between TS2 and the next INT2 in gas phase is practically the same as found in the previous case (2.0 vs 2.1 kcal/mol), but now it is more restrained in solvent (3.2 vs 4.4 kcal/mol).

TS3 lies below INT2 as before, but the presence of the larger substrate reduces the energy difference between them from 1.1 to 0.4 kcal/mol in gas phase and from 3.3 to 0.2 kcal/mol in protein environment. The calculated frequency of $88i$ cm^{-1} describes the proton shift from Glu111 residue to the amide nitrogen atom of the substrate and the simultaneous lengthening of peptide $N_1—C_1$ bond.

Finally, the product is obtained exothermically with an energy gain of 11.0 and 10.8 kcal/mol in the two phases, respectively. These two values are much more similar than those obtained in the path of Figure 4a, probably because in the presence of the bulky aliphatic side chains of substrate the active site is less accessible to the solvent.

The concordance of the results in the two examined cases, especially as far as the evaluation of the energetic barrier in the rate-limiting step of the reaction is concerned, suggests that reliable information can be obtained also by using a model for the substrate. In fact, at least in the present case, the removal of the side chains from substrate present in the PDB does not entail significant variations in the catalytic behavior of the enzyme. However, we think that this is no accident but depends on the manner in which the model of substrate is realized. If this is made in the right way, apart from the reliability of the results that is the most important goal, the additional advantage of a computational cost reduction can be reached.

Conclusions

In this work, we have reported a B3LYP investigation of the possible reaction mechanism of hydrolysis of two short peptides by insulin-degrading zinc enzyme, whose active-site model was constructed on the basis of crystal structure. The model, which consists of 130 or 159 atoms depending on the peptide length and has a total charge equal to zero, was built up large enough to allow reliable results. All stationary points along the reaction path were localized and characterized in gas phase and in protein environment. Results common to both examined cases can be summarized as follows:

The enzyme carries out its catalytic function through three fundamental steps that involve first a nucleophilic attack by a zinc-bound hydroxide to a substrate carbon. After a structural rearrangement of the key Glu111 residue that works as a shuttle, a proton is transferred onto an amide nitrogen of substrate and the peptide C−N is broken.

The role of amino acid residues suggested by previous experimental studies was fully confirmed by our results, from which can be deduced their active participation in the catalytic process or their presence as anchorage points for substrate and/or stabilization factors.

The rate-determining step of the reaction is the nucleophilic addition that implies an expense of 17.2 (15.7) kcal/mol, which is reduced to 15.9 (15.6) kcal/mol in protein medium when the shorter (longer) peptide substrates are considered. Calculations indicate that the next chemical events along the path are fast and lead to a product more stable than the starting enzyme−substrate complex by about 7.0 (11.0) kcal/mol in gas phase and 12.8 (10.8) in solvent for the first and second substrate, respectively.

The reliability of the model used to simulate the substrate was ascertained by calculations taking into account the real substrate as in the PDB structure. The similarity of the obtained results indicates that approximation of side chains with methyl groups is valid and allows a significant reduction of computational time.

The agreement with the unfortunately scarce experimental information concerning the working mechanism of this enzyme can be considered a sufficient validation for the theoretical approach used here, together with the fact that it was widely used previously for studying enzymatic reactions.

To our knowledge, this is the first investigation providing details on the mechanistic working of these types of enzymes. Thus, we hope that it will be used to stimulate future theoretical and experimental improvements.

Acknowledgment. We gratefully acknowledge the Dipartimento di Chimica, Università della Calabria, for financial aid.

Supporting Information Available: Three figures showing optimized structure of the enzyme−CH_3NH-Leu-Tyr-Leu-$CONHCH_3$ substrate complex and its stationary points (TS1, INT1, TS2, INT2, TS3, and PROD) on the IDE energetic profile. This material is available free of charge via the Internet at http://pubs.acs.org.

JA9037142